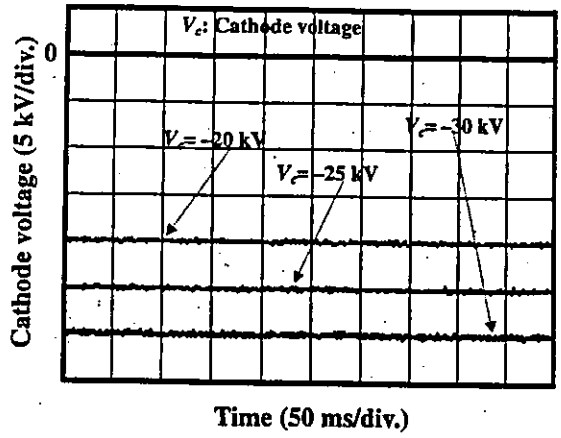

Fig. 5. Cathode voltages.

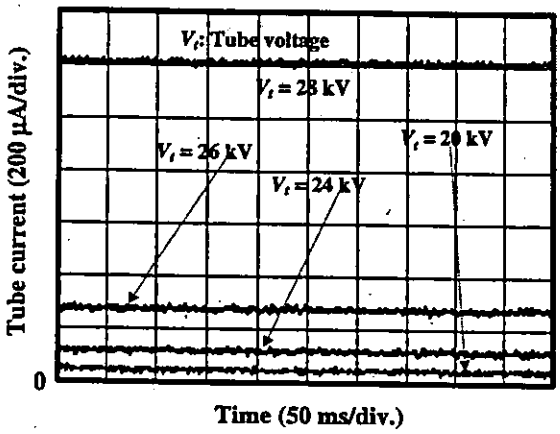

Fig. 6. Tube currents.

image contrast decreased somewhat with decreasing wire diameter due to blurring of the image caused by the sampling pitch, a 50-μm-diameter wire could be observed.

Figures 9 and 10 show angiograms of hearts. Iodine-based microspheres of 15 μm in diameter were used, and coronary

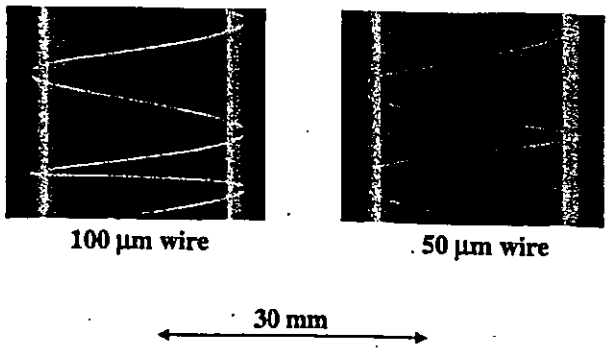

Fig. 8. Radiograms of tungsten wires of 50 and 100 μm diameter coiled around a pipe made of polymethyl methacrylate with tube voltage of 25 kV and exposure time of 20 s.

arteries and fine blood vessels of approximately 100 μm diameter were visible.

5. Discussion

In summary, we developed a simple X-ray generator with the cold-cathode diode and succeeded in producing characteristic molybdenum K-series X-rays using the transmission target as the K-edge filter. Subsequently, we confirmed the filtering effect of the target, and bremsstrahlung X-rays with photon energies higher than the edge were rarely detected with a tube voltage of 23 kV.

The current density J (A/cm^2) under field emission is written as:

$$J = 1.54 \times 10^{-6}(V/d)^2 \cdot \exp(-6.8 \times 10^7 \phi^{1.5} d/V)/\phi, \quad (1)$$

where V (V) is the tube voltage, d (cm) is the target-cathode distance, and ϕ (V) is the work function of the cathode element. Therefore, the current values in Fig. 6 corresponded qualitatively to eq. (1).

During the X-ray exposure, although the tube current decreases slightly due to ion sputtering, stable current flow can be obtained by selecting the appropriate cathode material and by controlling the radius of curvature of the cathode tip. In addition, the generator-produced number of

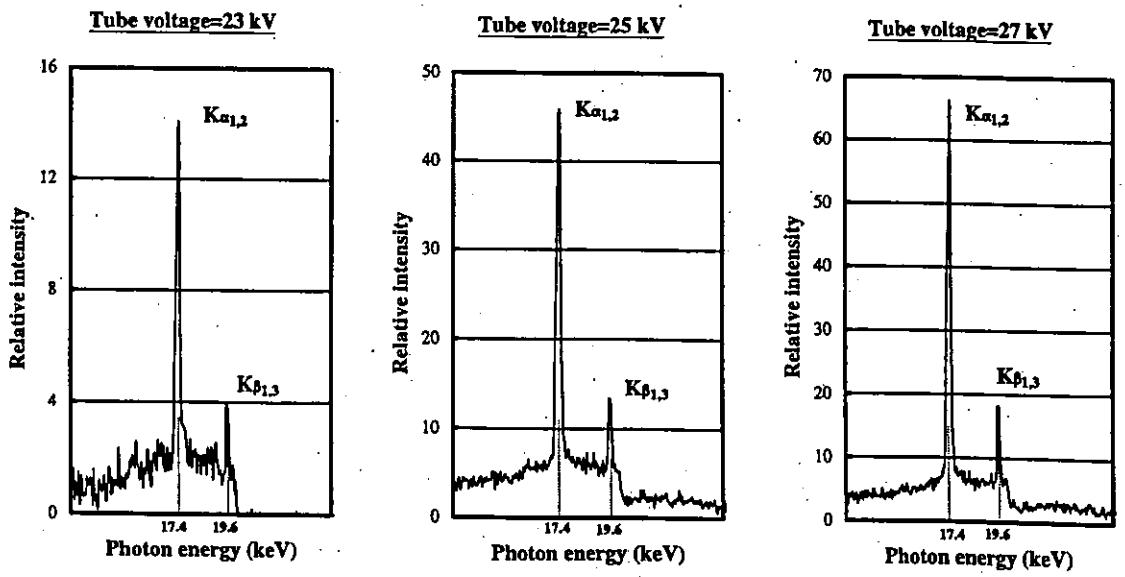

Fig. 7. X-ray spectra.

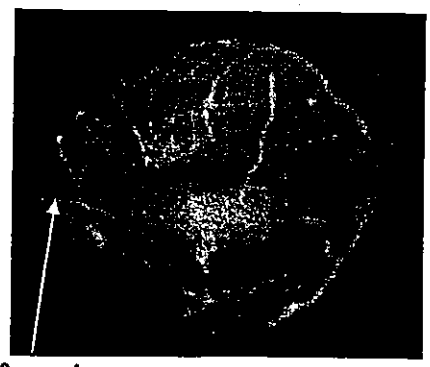

Fig. 9. Angiogram, using iodine microspheres, of extracted rabbit heart. Tube voltage and exposure time were 25 kV and 20 s, respectively.

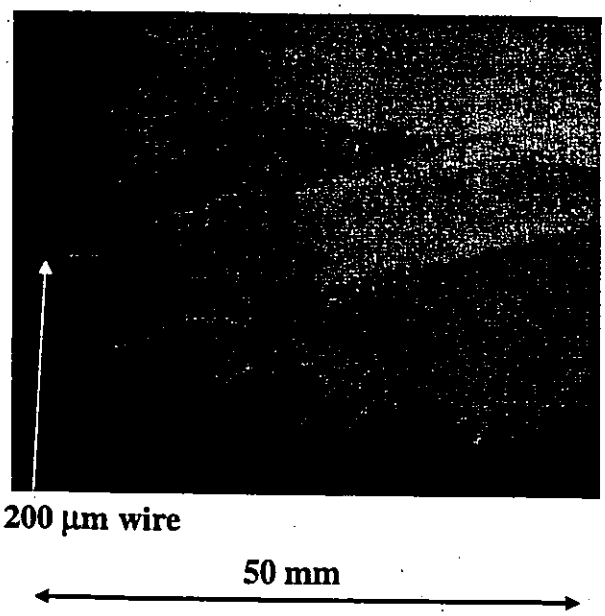

Fig. 10. Angiogram of extracted dog heart with tube voltage of 25 kV and exposure time of 60 s.

characteristic photons was approximately 4×10^6 photons/$cm^2 \cdot s$ at 1.0 m from the source with a tube voltage of 25 kV, and the photon count rate could be increased easily by increasing the tube voltage and current.

The focal spot dimensions decrease with decreasing target-cathode space, and the distance between the X-ray source and the imaging plate should be increased as much as possible to improve the spatial resolution. In soft radiography achieved with characteristic molybdenum K-series X-rays, because an X-ray lens such as a polycapillary plate[18] can be employed, the spatial resolution may be improved by decreasing the inner capillary diameter.

Under the pulsed operation, the high-voltage durability increases substantially, and both the size of the X-ray tube and the diameter of the high-voltage coaxial cable can be decreased. In this case, because the time-average tube current is regulated by the pulse repetition rate, both the tube voltage and the current can be controlled without using a hot cathode.

Recently, we developed a cerium-target X-ray tube to perform enhanced K-edge angiography utilizing cerium Kα rays (34.6 keV), since the rays are absorbed effectively by iodine-based contrast media with a K-edge of 33.2 keV. In addition, Kα rays from ytterbium (52.0 keV), tantalum (57.1 keV), and tungsten (58.9 keV) targets are very useful for performing K-edge angiography using gadolinium-based contrast media with an edge of 50.2 keV. Hence, using these rays, because the absorbed dose can be decreased effectively, extremely low-dose angiography can be accomplished.

Acknowledgment

This work was supported by Grants-in-Aid for Scientific Research (13470154, 13877114, and 16591222) and Advanced Medical Scientific Research from MECSST, Grants from Keiryo Research Foundation, The Promotion and Mutual Aid Corporation for Private Schools of Japan, JST, NEDO, and MHLW (HLSRG, RAMT-nano-001, RHGTEFB-genome-005, and RGCD13C-1).

1) A. C. Thompson, H. D. Zeman, G. S. Brown, J. Morrison, P. Reiser, V. Padmanabahn, L. Ong, S. Green, J. Giacomini, H. Gordon and E. Rubenstein: Rev. Sci. Instrum. **63** (1992) 625.
2) H. Mori *et al.*: Radiology **201** (1996) 173.
3) K. Hyodo, M. Ando, Y. Oku, S. Yamamoto, T. Takeda, Y. Itai, S. Ohtsuka, Y. Sugishita and J. Tada: J. Synchrotron Rad. **5** (1998) 1123.
4) T. J. Davis, D. Gao, T. E. Gureyev, A. W. Stevenson and S. W. Wilkins: Nature **373** (1995) 595.
5) A. Momose, T. Takeda, Y. Itai and K. Hirano: Nature Medicine **2** (1996) 473.
6) M. Torikoshi, T. Tsunoo, M. Sasaki, M. Endo, Y. Noda, T. Kohno, K. Hyodo, K. Uesugi and N. Yagi: Phys. Med. Biol. **48** (2003) 673.
7) F. E. Carroll, M. H. Mendenhall, R. H. Traeger, C. Brau and J. W. Waters: Am. J. Roentgenol. **181** (2003) 1197.
8) R. Germer: J. Phys. E: Sci. Instrum. **12** (1979) 336.
9) E. Sato, H. Isobe and F. Hoshino: Rev. Sci. Instrum. **57** (1986) 1399.
10) A. Shikoda, E. Sato, M. Sagae, T. Oizumi, Y. Tamakawa and T. Yanagisawa: Rev. Sci. Instrum. **65** (1994) 850.
11) K. Takahashi, E. Sato, M. Sagae, T. Oizumi, Y. Tamakawa and T. Yanagisawa: Jpn. J. Appl. Phys. **33** (1994) 4146.
12) E. Sato, K. Takahashi, M. Sagae, S. Kimura, T. Oizumi, Y. Hayasi, Y. Tamakawa and T. Yanagisawa: Med. & Biol. Eng. & Comput. **32** (1994) 289.
13) E. Sato, Y. Hayasi, R. Germer, E. Tanaka, H. Mori, T. Kawai, T. Ichimaru, S. Sato, K. Takayama and H. Ido: J. Electron Spectrosc. & Related Phenom. **137–140** (2004) 713.
14) E. Sato, Y. Hayasi, R. Germer, E. Tanaka, H. Mori, T. Kawai, T. Ichimaru, K. Takayama and H. Ido: Rev. Sci. Instrum. **74** (2003) 5236.
15) E. Sato, Y. Hayasi, R. Germer, E. Tanaka, H. Mori, T. Kawai, H. Obara, T. Ichimaru, K. Takayama and H. Ido: Jpn. J. Med. Phys. **20** (2003) 123.
16) H. Sugie, M. Tanemura, V. Filip, K. Iwata, K. Takahashi and F. Okuyama: Appl. Phys. Lett. **78** (2000) 2578.
17) E. Sato, K. Sato and Y. Tamakawa: Ann. Rep. Iwate Med. Univ. Sch. Lib. Arts Sci. **35** (2000) 13.
18) E. Sato, Y. Hayasi, R. Germer, E. Tanaka, H. Mori, T. Kawai, T. Ichimaru, S. Sato, K. Takayama and H. Ido: J. Electron Spectrosc. Related Phenom. **137–140** (2004) 705.

Available online at www.sciencedirect.com
SCIENCE DIRECT®
Biomaterials 24 (2003) 1223–1232
Biomaterials
www.elsevier.com/locate/biomaterials

Accelerated cell sheet recovery by co-grafting of PEG with PIPAAm onto porous cell culture membranes

Oh Hyeong Kwon[1], Akihiko Kikuchi, Masayuki Yamato, Teruo Okano*

Institute of Advanced Biomedical Engineering and Science, Tokyo Women's Medical University, 8-1 Kawadacho, Shinjuku, Tokyo 162-8666, Japan

Received 4 June 2002; accepted 30 September 2002

Abstract

Fabrication of functional tissue constructs from designed three-dimensional structures of cells using the layered method of cultured cell sheets could prove to be an attractive approach to tissue engineering. Rapid recovery of cell sheets is considered to be important as a basic technology for practical assembly of tissue-mimicking structures. To accelerate required culture substrate hydrophilic/hydrophobic functional changes according to the hydrated/dehydrated structural changes in response to culture temperature alteration, poly(*N*-isopropylacrylamide) (PIPAAm) was grafted with poly(ethylene glycol) (PEG) onto porous culture membranes by electron beam irradiation. Analyses by attenuated total reflection-Fourier transform infrared and electron spectroscopy for chemical analysis revealed that PIPAAm and PEG were successfully grafted to surfaces of porous membranes. PIPAAm-grafted porous membranes (PIPAAm-PM) were compared with porous membranes co-grafted with various amounts of PEG and PIPAAm (PIPAAm(PEG)-PM) for cell sheet detachment experiments. Approximately 35 min incubation at 20°C was required to completely detach cell sheets from PIPAAm-PM in a static condition, while only 19 min to detach cell sheets from PIPAAm(PEG0.5%)-PM, which is co-grafted with PIPAAm and 0.5 wt% of PEG. With porous membranes, water molecules were accessed by the PIPAAm molecules grafted on the surfaces from both underneath and peripheral to the attached cell sheet, resulting in more rapid hydration of grafted PIPAAm molecules and detachment of cell sheet than that for nonporous tissue culture polystyrene (TCPS) dish. With PIPAAm(PEG)-PMs, grafted PEG chains should accelerate the diffusion of water molecules to PIPAAm grafts, showing more rapid detachment of cell sheet compare to PIPAAm-PMs.

Keywords: Bovine aortic endothelial cells; Poly(*N*-isopropylacrylamide); Poly(ethylene glycol); Porous membrane; Hydration; Rapid cell detachment

1. Introduction

Rapid detachment of intact cultured cell sheets is very important to fabricate a functional tissue-mimicking structure by stratification of detached cell sheets. To recover intact cell sheets from culture surfaces, we have prepared tissue culture polystyrene (TCPS) dishes grafted with poly(*N*-isopropylacrylamide) (PIPAAm) [1–5]. PIPAAm shows lower critical solution temperature (LCST) in aqueous solution at 32°C. PIPAAm is soluble in water below 32°C while it becomes insoluble above this temperature [6] due to the hydration changes around isopropyl side groups. Incorporating PIPAAm onto a solid surface showed hydrophilic–hydrophobic surface property alterations responding to temperature changes [7,8]. We utilized the temperature responsive surface property alteration to culture and recover cells from these surfaces [1–5]. Confluent culture of cells forms on these surfaces, and we have successfully recovered intact, viable monolayer cell sheets to construct three-dimensional tissue-like structures. The hydrophobic, collapsed PIPAAm-grafted surface above the PIPAAm's LCST becomes hydrophilic by only decreasing culture temperature below the LCST.

We have already reported that cells cultured on TCPS surfaces grafted with PIPAAm can be recovered

*Corresponding author. Tel.: +81-33353-8111x30233; fax: +81-33359-6046.
E-mail address: tokano@abmes.twmu.ac.jp (T. Okano).
[1] Present address. Department of Polymer Science and Engineering, Kumoh National Institute of Technology, 188 Shinpyung-dong, Kumi, Kyungbuk 730-701, Korea.

0142-9612/02/$ - see front matter © 2002 Elsevier Science Ltd. All rights reserved.
PII: S0142-9612(02)00469-6

by reducing temperature without enzymatic treatment [1–3]. In our previous reports, we have described the recovery of bovine aortic endothelial cell sheets from PIPAAm-grafted TCPS surfaces [4], and also showed that cell sheets are recovered together with their deposited fibronectin matrix by low temperature treatment [5].

Recently, we succeeded in harvesting designed human aortic endothelial cell sheets noninvasively from the PIPAAm-grafted surfaces and transferring them onto other surfaces [9]. Furthermore, Madin–Darby canine kidney (MDCK) cell sheets were easily transferred from PIPAAm-grafted surfaces to other culture dishes by utilizing hydrophilic poly(vinylidene difluoride) membranes as supporting materials during the transfer procedure [10]. The recovered cell sheets attached easily to other surfaces and started to proliferate again probably due to the recovered extracellular matrices including the fibronectin component accompanied with detaching cell sheet. This two-dimensional cell sheet manipulation technique could be proven attractive to construct three-dimensional tissue-like structures by layering detached cell sheets obtained from different cell types, i.e., endothelial cells, hepatocytes, kidney cells, and so on.

However, spontaneous cell sheet detachment from surfaces of PIPAAm-grafted TCPS is relatively a slow process, occurring gradually from the sheet periphery toward the interior. Thus, significant incubation time at reduced temperature is required to lift up an intact cell sheet completely. Rapid detachment of cultured cell sheets is a very important recovery method that permits facile manipulation of the sheets.

The rate-limiting step to cell sheet recovery is the hydration of the underlying PIPAAm molecules grafted on the surface. To accelerate the hydration of the hydrophobized PIPAAm segments interacting with the cell sheet, incorporation of a highly water permeable substrate to interface is desirable between the cell sheets and the thermoresponsive polymer surfaces. Recently, we have reported that the use of porous membranes grafted with PIPAAm as culture substrates facilitated the rapid cell sheet detachment [11]. Incorporation of PEG graft side chains into PIPAAm hydrogels resulted in the accelerated gel swelling–deswelling characteristics while maintaining the polymer transition temperature as was observed for homopolymer IPAAm [12,13]. This is probably due to the formation of water releasing channels with the grafted PEG chains. Thus, the introduction of PEG-grafted chains onto PIPAAm-grafted surfaces could lead to more rapid hydration of the cell culture surfaces. In the present study PEG chains were co-grafted with PIPAAm onto porous membranes to achieve a much more rapid cell sheet detachment than porous membrane grafted with only PIPAAm.

2. Materials and methods

2.1. Materials

N-isopropylacrylamide (IPAAm) was kindly provided by Kohjin (Tokyo, Japan) and used after recrystallization from *n*-hexane. PEG methacrylate (MW = 4000) was a kind gift from NOF Co. (Tokyo, Japan). Tissue culture-grade polystyrene dishes (TCPS, Falcon 3001) and Cell Culture Inserts™ (Falcon 3090) with a microporous poly(ethylene terephthalate) membrane (pore size = 0.45 μm, pore density = $1.6 \times 10^6/cm^2$, surface area = $4.2\,cm^2$) were purchased from Becton Dickinson Labware (Oxnard, CA, USA). Trypsin-EDTA solution, streptomycin, and penicillin were obtained from Gibco BRL (Grand Island, NY, USA). Dulbecco's modified Eagle's medium (DMEM) was purchased from Iwaki (Chiba, Japan).

2.2. Preparation of PIPAAm(PEG)-PM

PIPAAm(PEG)-PM used for single cell culture and cell sheet recovery was prepared by the procedure as previously reported [11]. The procedure is briefly described as follows: IPAAm monomer and various amounts of PEG macromonomer were dissolved in 2-propanol containing 0.05% distilled water at a total concentration of 60 wt/wt%. This monomer solution (30 μl) was spread uniformly over the surface of a porous membrane (Cell Culture Insert™). An electron beam was immediately irradiated using an Area Beam Electron Processing System (Curetron EBC-200-AA2, Nissin-High Voltage Co. Ltd., Kyoto, Japan) at a radiation dose of 0.3 MGy with acceleration voltage of 150 kV under 1.0×10^{-4} Pa. IPAAm monomer and PEG macromonomers were polymerized and covalently grafted onto the porous membrane simultaneously by this electron beam irradiation. Unreacted monomers and ungrafted polymers were removed by extensive washing with cold water. Polymer-grafted porous membranes were dried in vacuo at room temperature. PIPAAm-PM was also prepared by the same method as described above using IPAAm monomer alone.

2.3. Surface characterization

The amounts of PIPAAm grafted onto porous membranes were determined by ATR-FTIR (JASCO Valor-III, Tokyo, Japan) [4,11]. The control substrates, porous poly(ethylene terephthalate) membranes, have strong absorption band attributed to ester carbonyl bond at $1720\,cm^{-1}$. As PIPAAm was grafted onto each substrate, an amide carbonyl absorption band appeared in the region of $1650\,cm^{-1}$. The peak intensity ratio ($I_{1650/1720}$) was used to determine the amount of PIPAAm grafted on each surface using a calibration

curve of known PIPAAm amount cast on the porous membrane from the solution.

All the sample surfaces were also analyzed using the ESCA (PHI 5800 ESCA system, Physical Electronics, MN, USA). Survey spectra were acquired with a take-off angle of 90° and surface elemental compositions were calculated from integrated peak areas for each element.

An AFM (NanoScope IIIa, Digital Instruments Inc, CA, USA) was utilized to scan the surface topography. All samples were analyzed in dry state and examined in Tapping Mode™ with a commercial silicon nitride cantilever. The scan size of each surface was 2.6 μm × 2.6 μm. The detection angle and scan speed were 90°and 1 Hz, respectively.

2.4. Contact angle measurements

Six samples each of PIPAAm-PM, PIPAAm-(PEG0.1%)-PM, PIPAAm(PEG0.5%)-PM, and ungrafted PM were cut in size (1.5 × 0.8 cm) to measure water contact angles. The water contact angles were determined by the sessile-drop method at 20°C and 37°C with a FACE contact angle meter (Image processing type CA-X, Kyowa Interface Science, Saitama, Japan) connected with circulating thermostated water bath. All samples were measured six times and averaged. Contact angles at 20°C and 37°C were presented as a mean value ($n = 6$) with standard deviation.

2.5. Cell culture

Bovine aortic endothelial cells (BAECs) were purchased from Clonetics Co. (MD, USA) and cultured on TCPS dishes using DMEM supplemented with 10% FBS, 100 units/ml of penicillin, and 100 μg/ml of streptomycin at 37°C in a humidified atmosphere with 5% CO_2. BAECs were recovered from ungrafted TCPS dishes by treatment with 0.25% trypsin–0.26 mM EDTA in PBS and subcultured on ungrafted TCPS dishes, and each modified surface. The cell morphology was monitored and photographed periodically under phase-contrast microscopy (TE300, Nikon, Tokyo, Japan) equipped with Nikon F70 camera.

2.6. Detachment of single endothelial cells

Detachment of single endothelial cell was achieved using low temperature treatment after incubation at 37°C for 3 h. BAECs were plated on each surface at a density of 3×10^4 cells/cm^2 and cultured for 3 h to allow attachment and spreading on each polymer-grafted surface. For low temperature treatment, the spread cells were transferred to a CO_2 incubator equipped with a cooling unit fixed at 20°C. After 5, 10, 15, 20, 30 and 45 min incubation, cell morphology was observed using a phase-contrast microscope and photographed. Both rounded and spread cells in the photographs were counted, and the percentage of the rounded cells to the total cells counted was presented as the mean value with standard deviation in four observation areas. Ungrafted porous membranes were used as controls. The percent recovery of single cells from PIPAAm(PEG0.1%)-PMs and PIPAAm(PEG0.5%)-PMs was compared to PIPAAm-PM and ungrafted PM surfaces.

2.7. Detachment of confluently cultured endothelial cell sheets

BAECs were plated onto each surface at a density of 1.3 times that of the confluence (1.3×10^6 cells/dish) and cultured at 37°C. After 24-h cultivation, unattached cells were removed by medium change. Cells were cultured for 8 days after reaching confluence, and each plate was transferred to the CO_2 incubator equipped with a cooling unit fixed at 20°C, and periodically taken out from incubator to acquire photographs during detachment with care to avoid longer time exposure at ambient temperature. All procedures were carefully carried out not to alter the incubator temperature because the cell culture surfaces used in this experiment are all thermoresponsive. The photographs were scanned into a computer system for analysis. Software, NIH Image (version 1.61) for Macintosh was used to measure the area of each detached cell sheet. Areas of detached cell sheets relative to in situ confluently cultured cell monolayer area were calculated and averaged from four photographs of each sample.

2.8. Statistical analysis

All the data obtained were expressed as the mean with standard deviation and analyzed using student's t-test.

3. Results and discussion

3.1. Surface characterization

Elemental analyses of porous membrane surfaces grafted with PIPAAm, co-grafted with PEG and PIPAAm, and ungrafted PM were carried out using ESCA, and surface compositions are summarized in Table 1. Increased atomic percent of nitrogen was observed on PIPAAm-PM, PIPAAm(PEG0.1%)-PM and PIPAAm(PEG0.5%)-PM surfaces after electron beam irradiation. As control PET porous membrane surface does not contain nitrogen atom in its chemical structure, these results directly support PIPAAm grafting onto porous membrane by electron beam irradiation. Furthermore, introduction of PEG chains on porous membranes was confirmed by the increase in

Table 1
Atomic composition of ungrafted, PIPAAm-grafted, and PIPAAm with various amounts of PEG-grafted porous membrane surfaces determined by ESCA

Substrate	Atom (%)[a]			
	C	O	N	N/C
PM	72.7±1.7	26.9±1.5	0.4±0.2	0.006±0.003
PIPAAm-PM	75.5±1.4	17.3±1.2	7.2±0.7	0.095±0.010
PIPAAm(PEG0.1%)-PM	73.0±1.6	21.2±1.7	5.8±0.5	0.079±0.007
PIPAAm(PEG0.5%)-PM	70.9±1.6	24.1±1.5	5.0±0.3	0.070±0.005

[a] Data are expressed as the mean of three samples with standard deviation.

oxygen content on PIPAAm(PEG0.1%)-PM and PIPAAm(PEG0.5%)-PM surfaces. The oxygen content on the latter surface is slightly higher than on the former one. Amounts of PIPAAm grafted onto porous membranes determined by comparison with ATR-FTIR standard curves are presented in Table 2. All the samples had consistent surface amounts of grafted PIPAAm, which enabled direct comparison of detachment of cells and cell sheets from each modified surface.

Table 3 shows water contact angle data from each surface using the sessile-drop method at 20°C and 37°C. PIPAAm-grafted surfaces exhibited decreasing contact angles by lowering temperature from 37°C to 20°C, while control PET surfaces had negligible contact angle changes with temperature. This result indicates that PIPAAm surfaces, relatively hydrophobic at higher temperature, became more hydrophilic in response to temperature reduction due to spontaneous hydration of surface-grafted PIPAAm molecules [1–5]. We previously reported quite large contact angle changes of PIPAAm-modified glass plate surfaces [7,8]. Large contact angle changes observed for PIPAAm-grafted surfaces were due to the existence of free mobile chain end of linear PIPAAm grafts on the surfaces. Electron beam irradiation used for PIPAAm-grafted culture dish preparation caused cross-linking reaction within the grafted PIPAAm chains in part, restricting PIPAAm chain mobility. Thus, the contact angle changes observed on PIPAAm-PM were at the most 10°. This difference is sufficient to enable cell detachment by low temperature treatment. Tamada and Ikada [14] reported that water contact angles of material surfaces strongly influence cell attachment behavior, and show maximum cell attachment around 60° of contact angle. In our system, surface wettability at 37°C should be suitable for cell attachment as judged from contact angle data, hydration of the surface-grafted PIPAAm chains might affect detaching of cultured cells at 20°C. There are negligible contact angle differences between PIPAAm-PM, PIPAAm-(PEG0.1%)-PM and PIPAAm(PEG0.5%)-PM surfaces above the LCST, despite the introduction of PEG chains. This result suggests that, above the LCST, grafted PEG chains scarcely exist in the outermost of the

Table 2
Amount of grafted PIPAAm on each porous membrane determined by ATR-FTIR

Substrate	Grafted PIPAAm[a] (μg/cm²)
PM	None
PIPAAm-PM	2.0±0.4
PIPAAm(PEG0.1%)-PM	1.8±0.4
PIPAAm(PEG0.5%)-PM	2.1±0.2

[a] Data are expressed as the mean of four samples with standard deviation.

Table 3
Water contact angle changes of the PIPAAm-grafted, PIPAAm with various amount of PEG-grafted, and ungrafted porous membrane surfaces with temperature as estimated by sessile-drop method

Substrate	θ_{H_2O}[a]	
	20°C	37°C
PM	58.0±2.7	59.1±3.1
PIPAAm-PM	50.7±2.6	58.1±3.4
PIPAAm(PEG0.1%)-PM	44.7±1.8	57.1±2.6
PIPAAm(PEG0.5%)-PM	41.1±2.3	57.6±1.7

[a] Data are expressed as the mean of six samples with standard deviation.

membrane surfaces due to the hydrophobically contracted PIPAAm chains, i.e., rearrangement of PEG chains was highly suppressed by the hydrophobically aggregated PIPAAm chains. In the case of PIPAAm-(PEG)-PM surface, it was found that the change in water contact angle was larger with temperature change compared to that for PIPAAm-PM surface, and increased slightly for PIPAAm(PEG0.5%)-PM (57–41°), containing 0.5 wt% PEG compared to that for PIPAAm(PEG0.1%)-PM (58–44°) containing 0.1 wt% PEG. This means that embedded PEG chains interior of contracted, dehydrated PIPAAm network with limited mobility regained their freedom through hydration by reducing temperature leading to rearrangement of PEG chains to the membrane surfaces and increase of surface

hydrophilicity. By lowering temperature, such a hydrophobic to hydrophilic polymer property alteration and polymer matrix swelling induced the detachment of cultured cells from PIPAAm-grafted surfaces [1–3]. Especially, grafted PEG chains might contribute to the rapid cell and/or cell sheet recovery by virtue of increased contact angle change as shown in Table 3.

The three-dimensional AFM images of PIPAAm-PM, PIPAAm(PEG0.5%)-PM, and ungrafted PM revealed that porous membrane surfaces grafted with PIPAAm by electron beam irradiation retained their microporous structure (Fig. 1). Surfaces of ungrafted control porous membranes had relatively rougher topography, while those of PIPAAm-PM and PIPAAm(PEG0.5%)-PM were much smoother. Surface roughness for each surface was estimated by digital AFM autocalculation over a $2.6 \times 2.6\,\mu m$ section excluding the porous part. Mean roughness values for PIPAAm-PM, PIPAAm-(PEG0.5%)-PM, and ungrafted PM were 4.1 ± 0.5, 4.3 ± 0.6, and 6.1 ± 0.5 nm, respectively. This indicated that grafted PIPAAm on porous membranes had covered and smoothened relatively rougher control surfaces. A negligible difference of surface roughness existed between PIPAAm-PM and PIPAAm-(PEG0.5%)-PM surfaces, although PEG chains were co-grafted with PIPAAm for PIPAAm(PEG0.5%)-PM, probably due to the small amount of PEG chains interior of the dehydrated PIPAAm network.

3.2. Cell culture

BAECs were well attached and spread on all the sample surfaces within 1 h incubation at 37°C. After 3-h incubation at 37°C, almost all of the seeded cells were attached and spread on those surfaces, despite the porosity of the membrane surfaces. Used porous membranes here had a pore size of 0.45 μm in diameter, much smaller than the size of a single cell. Therefore, cells appeared to override these surface discontinuities produced by track-etched pores without difficulty [11,15]. Cell attachment and spreading on PIPAAm-PM, PIPAAm(PEG0.1%)-PM, PIPAAm(PEG0.5%)-PM, and ungrafted control PM surfaces were nearly identical (data not shown).

Poly(ethylene glycol) has received wide recognition as a biomaterial because of its unique adhesive resistance properties for biomolecules and cells [16,17]. Its lack of interaction with proteins and other biological entities

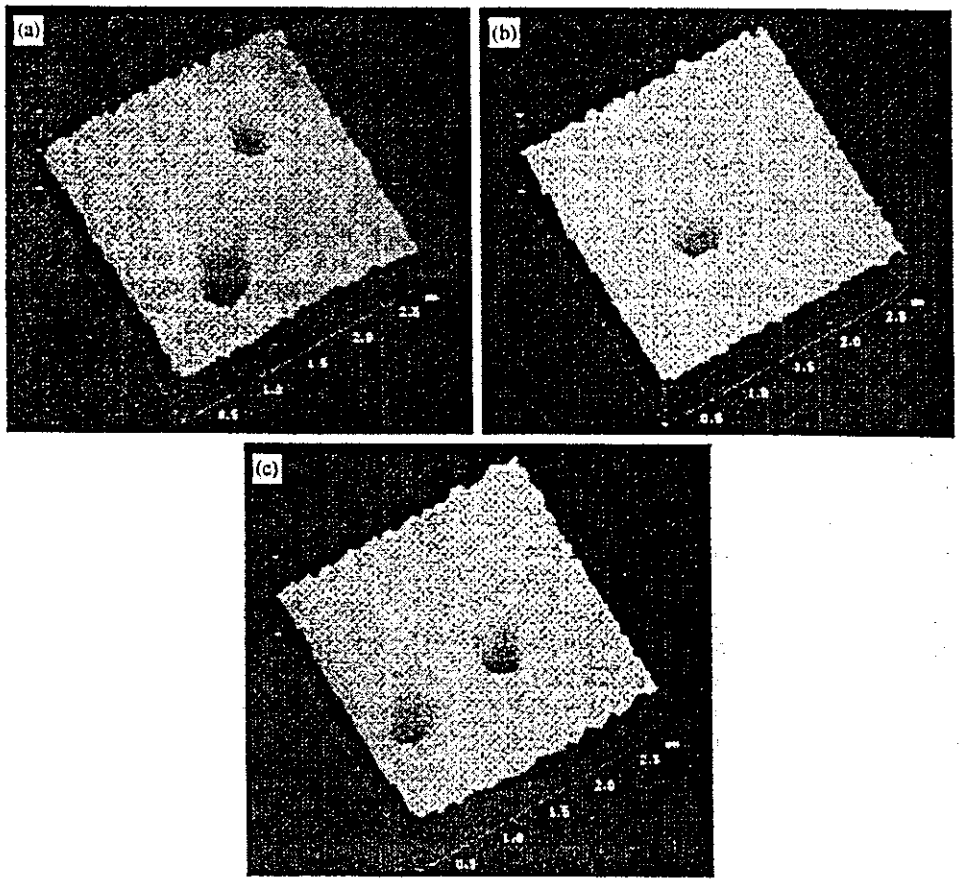

Fig. 1. Three-dimensional images for surfaces of: (a) a control PM, (b) PIPAAm-PM and (c) PIPAAm(PEG0.5%)-PM obtained by tapping mode AFM. Pore of 0.45 μm diameter is shown in each image.

makes it a promising material for use in many biomedical applications [18–21]. Generally, PEG-grafted surfaces show nonfouling property, because of the unique properties including low PEG–water interfacial energy [22], high PEG chain mobility [23,24], high water content of PEG gels, water structuring by PEG chains as well as exclusion volume effects [25,26]. Because of these properties cells do not adhere on PEG-grafted surfaces.

Nakayama et al. [27] prepared PET films coated with PEG-polystyrene amphiphilic block copolymers. When the film was immersed in water, the PEG blocks were oriented toward water phase which resulted in decreased cell adhesion due to the enhanced surface hydrophilicity. In our study, however, even PEG chains were co-grafted with PIPAAm onto porous membranes, PEG chains were embedded interior of dehydrated PIPAAm gel layers, which were suggested by the water contact angle data (Table 3). Actually, cell attachment was slightly suppressed on grafted surfaces with more than 1% of PEG chains, and could not form confluent monolayer cell cultures on the whole surface area (data not shown). This is probably because, in the case of high PEG content surface, some PEG chains existed on the surfaces to inhibit partially cell attachment and prevent complete coverage of all culture surfaces with proliferating cells.

3.3. Single cell detachment

When the culture temperature was reduced to 20°C after 3 h incubation at 37°C during which almost all of the seeded cells were attached and spread on those surfaces, the spread cells were rounded and detached from both the surfaces. This is because PIPAAm is hydrated below its LCST, producing an expanded, swollen, and hydrophilic surface. This surface property change weakened cellular adhesion, resulting in spontaneous cell detachment.

Fig. 2 shows the percentage of detached single cells from the surfaces of PIPPAm-TCPS dishes, PIPAAm-PMs, PIPAAm(PEG0.1%)-PMs, and PIPAAm-(PEG0.5%)-PMs as a function of lower culture temperature treatment time. There were no cells detached from ungrafted control porous membrane because of no surface property alteration by reducing the temperature. For the same reason, cells cultured on ungrafted nonporous TCPS dishes did not detach as expected [11]. The spread cells cultured on the PIPAAm-PM detached more rapidly than those on PIPAAm-TCPS dish. In the case of modified porous membranes water molecules for hydration of PIPAAm were supplied through pores underneath the adherent cells as well as from the periphery of each cell. By contrast, water molecules to hydrate PIPAAm chains on PIPAAm-TCPS dishes could readily penetrate the culture matrix

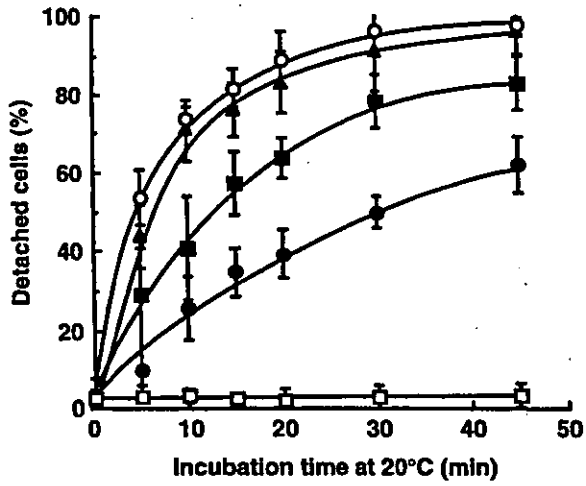

Fig. 2. The percentage of detached single cells from control PM surface (□), PIPAAm-TCPS surface (•), PIPAAm-PM (■), PIPAAm(PEG0.1%)-PM (▲) and PIPAAm(PEG0.5%)-PM (○) as a function of incubation time in culture medium at 20°C.

only from the periphery of each cell to the interface between the cell and grafted PIPAAm chains. When porous membranes were co-grafted with PEG and PIPAAm, the spread cells on PIPAAm(PEG)-PMs showed more rapid detachment behavior than on PIPAAm-PM surfaces. As shown in Fig. 2, cells spontaneously detached from PIPAAm(PEG0.1%)-PMs (43% of detachment) and PIPAAm(PEG0.5%)-PMs (53%) more rapidly than from PIPAAm-PM (29%) and PIPAAm-TCPS surfaces (10%) after initial 5 min incubation at 20°C. Approximately 45 min incubation below the LCST was required to detach nearly all the spread cells from porous membrane surfaces co-grafted with PEG and PIPAAm chains. PEG chains of highly hydrophilic and hygroscopic nature were able to enhance water diffusion to the entire PIPAAm grafts between the porous membrane and attached cells, i.e. more rapid and extensive water supply is achieved by co-grafting of PEG chains with PIPAAm. Rapid access of bulk water to PIPAAm grafts by the existence of PEG chains should accelerate single cell detachment. Detached cells adhere to and grow readily on other surfaces at 37°C. We already reported that cultured single hepatocytes were detached with pre-adsorbed fibronectin matrix by low temperature treatment from PIPAAm-TCPS surfaces as a result of physical cell contractile forces [28]. We also reported that the detached cells maintained their differentiated function, i.e., albumin secretion more than cells detached by trypsinization after re-adhesion because membrane proteins were readily degraded by enzymatic digestion which resulted in extremely low function of adhering and growing on the new surfaces [2]. Recovered extracellular matrices including fibronectin with cells are considered to enhance re-adhesion of recovered cells to other surfaces.

3.4. Cell sheet detachment

When culture temperature is decreased below the LCST after cells proliferate to confluency, cells spontaneously detach from the temperature-responsive PIPAAm grafted porous membranes with intact cell–cell junctions. The generally used enzymatic digestion method brings monolayer cell sheet to single cells, because membrane proteins and extracellular matrices are susceptible to destruction by usual enzymatic digestion. For example, even though keratinocytes can be obtained from the membrane of sheet configuration for transplantation to burned patients in clinical application, recovery of cultured sheets are usually carried out with dispase, which induces significant destruction of cadherin and extracellular matrix proteins [29]. This deterioration forced medical doctors to use antibiotics over the transplanted skin to avoid patients from infection.

Results shown in Fig. 2 suggest the possible detachment of two-dimensional cell sheets in a short time period using PIPAAm(PEG)-PM through which water is supplied both from underneath and the periphery of a cell sheet and enhanced water diffusion by co-grafted hydrophilic PEG moiety, resulting in rapid hydration of grafted PIPAAm molecules. Fig. 3 shows changes in detached area of cell sheets on PIPAAm-TCPS, PIPAAm-PM, PIPAAm(PEG0.1%)-PM, and PIPAAm(PEG0.5%)-PM as a function of reduced temperature treatment time. Cell sheets are observed to detach spontaneously and more rapidly from the PIPAAm-PM surfaces (~35 min) than nonporous PIPAAm-TCPS surfaces (~75 min) with a culture area of 4.2 cm^2 under quiescent culture conditions and reduced culture temperature. These results support that accelerated detachment of cell sheets is due to the existence of pores on membrane surface as previously reported [8]. Moreover, dramatically rapid cell sheet detachment was achieved from the PIPAAm(PEG)-PM surfaces. Cell sheets were completely detached from PIPAAm(PEG0.1%)-PM and PIPAAm(PEG0.5%)-PM surfaces within 23 and 19 min incubation, respectively, at reduced temperature. Medium temperature changes were monitored immediately after dish transfer from incubator set at 37°C to incubator set at 20°C. As the medium volumes were 2 ml for dish and 3 ml total for PIPAAm-PM insert placed dishes, temperature drop was slightly slower for PIPAAm-PM insert placed dishes; i.e., 5 min was required for normal dish, and 7 min for PIPAAm-PM insert dishes to re-equilibrium state at 20°C. Note that the medium temperature was lower than the PIPAAm's LCST after 1 min incubation at 20°C for each case. Although the temperature change was more rapid for normal dish, probably due to the volume difference, more pronounced cell sheet detachment was apparent for the case in porous membrane

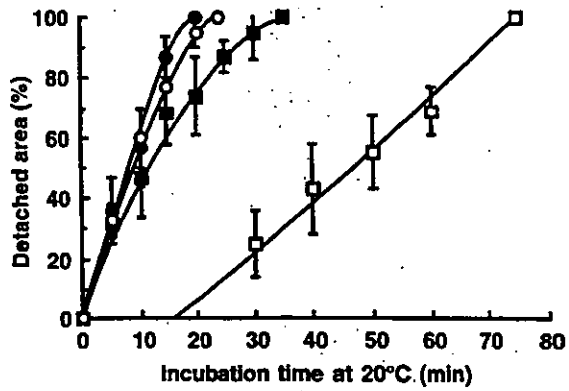

Fig. 3. Average detached areas for cell sheets recovered from PIPAAm-TCPS (□), PIPAAm-PM (■), PIPAAm(PEG0.1%)-PM (○) and PIPAAm(PEG0.5%)-PM (•) surfaces with culture area of 4.2 cm^2 as a function of incubation time in culture medium at 20°C.

with PEG chains co-grafted with PIPAAm on the surfaces. Considering that the amount of PIPAAm grafted on each surface is similar, and therefore, the degree of hydration force produced to detach adhered cells is also similar, the observed rapid cell sheet detachment from PIPAAm(PEG)-PM surfaces is significant. These results are probably attributed to the existence of co-grafted PEG moiety, which should accelerate cultured cell sheet detachment by effective, and enhanced diffusion of water molecules to cell–substrate interface to hydrate the graft chains of PIPAAm. We already reported that hydrophilic PEG grafts introduced into PIPAAm cross-linked network formed channels for water molecules to accelerate gel swelling/deswelling changes [12, 13].

Cell sheets on PIPAAm-grafted TCPS surfaces initially detached slowly, probably because the water required to hydrate grafted PIPAAm could only penetrate from the cell sheet periphery (Scheme 1a). Cell sheets on PIPAAm-PM surfaces detached more rapidly with onset of low temperature treatment, suggesting that PIPAAm-PM surfaces permit rapid rehydration by water penetration through pores beneath as well as the periphery of cell sheets at 20°C (Scheme 1b). Moreover, co-grafted PEG chains on PIPAAm-(PEG)-PM provide effective pathways of water molecules and their diffusion from micropores to PIPAAm grafts (Scheme 1c). This contrasting mechanism between each grafted surface is schematically depicted in Scheme 1.

Until now, we used the PIPAAm-grafted TCPS surfaces to detach cultured cell sheets at 20°C. Cell sheets formed on PIPAAm-grafted TCPS surfaces detach slowly and gradually, beginning from sheet edges and moving toward the cell sheet interior, presumably because water penetrates the interface between cell sheets and PIPAAm-grafted dish surfaces mainly from the periphery of cells (Scheme 1a). Chitin membranes

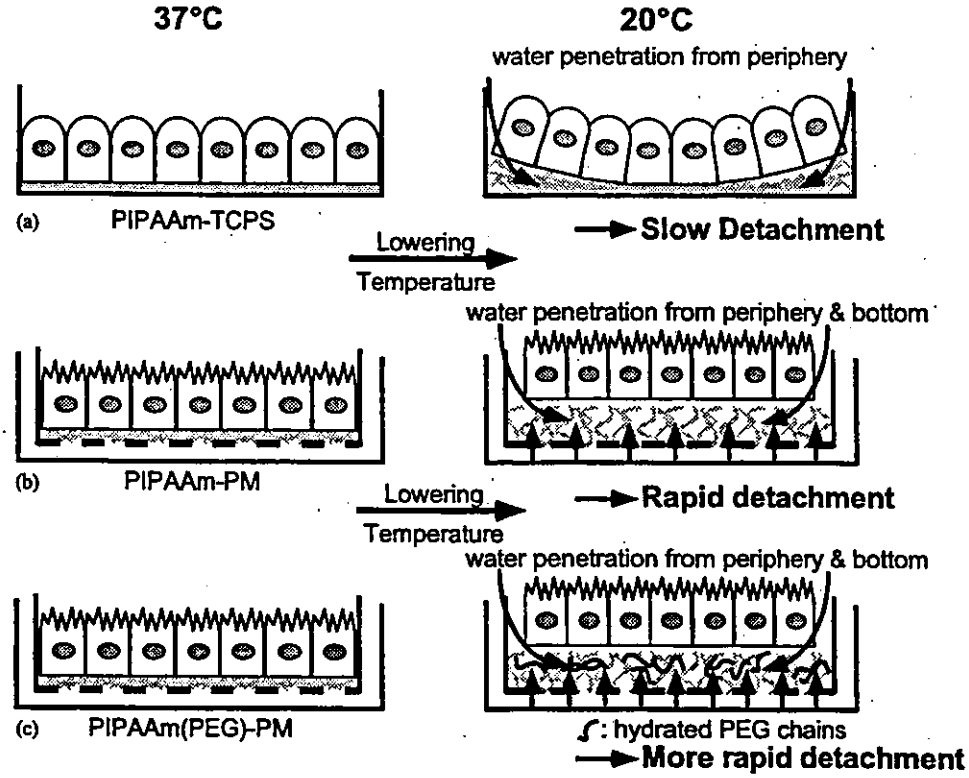

Scheme 1. Illustration of cell sheet detachment through different types of water supply to: (a) PIPAAm-TCPS dish, (b) PIPAAm-PM and (c) PIPAAm(PEG)-PM surfaces.

were used to detach and transfer cell sheets to other surfaces with maintained cell polarity [4]. When the cell sheets are detached from the culture surfaces, they readily tend to contract because of strong cell–cell interaction [30], therefore the use of chitin membranes as supporting materials enabled transferring of detached cell sheets without shrinkage. This idea was also applied to achieve rapid detachment of cultured cell sheets [9, 10]. In contrast to renal epithelial cell lines, MDCK cell sheets are detached from PIPAAm-grafted TCPS dishes merely by reduced temperature after 4 weeks of culture, such cell sheet detachments were greatly repressed in the early stages of culture (up to 3 weeks) probably because the contractile force of MDCK cells is weak. Recently, we succeeded in the rapid harvest of confluent MDCK cell sheet and intact transfer to other culture dishes by utilizing hydrophilic poly(vinylidene difluoride) (PVDF) membrane as a cell sheet mover [9,10]. The whole MDCK cell sheet was harvested together with the PVDF membrane because the PVDF membrane stuck to apical cell surfaces by physical attraction force. Below the LCST, the interaction between apical cell surfaces and the PVDF membrane should be higher than that between basal cell surfaces and hydrated PIPAAm surfaces. In the present report, however, we tried to achieve rapid cell sheet detachment under quiescent culture condition and reduced temperature without any supporting materials. If some supporting materials like a PVDF membrane are used, cell sheets might detach much more rapidly than those under the quiescent culture condition from the PIPAAm(PEG)-PM surfaces.

Previously, we have succeeded in fabricating stratified cell sheet culture by two-dimensional cell sheet manipulation to construct tissue-like structures [31]. In natural organs, the parenchyma comprises intimately associated cell sheets. Liver comprises basically two sheets of hepatocytes and endothelial cells those are interconnected to form a continuous three-dimensional tissue. To construct liver lobule structure, the basic unit of liver, hepatocytes and endothelial cells were cultured separately on PIPAAm-grafted TCPS dishes. Cultured confluent monolayer cell sheets of hepatocytes were detached by low temperature treatment and placed onto a confluent endothelial cell sheet. Stratified cell sheets are highly resembled liver lobules histologically. Intact, viable cell sheet detachment by lower temperature treatment could prove useful to construct three-dimensional tissue-like structures by fabricating sandwiches of cell sheets and associated ECM for application to tissue restoration, as a transplant material, or for construction of artificial organs. Thus, rapid detachment and recovery methods are needed to maintain cell phenotype and biological functions. Porous membranes co-grafted

with PEG and thermoresponsive PIPAAm are shown to be capable of achieving such dramatically rapid two-dimensional cell sheet detachment.

4. Conclusions

Porous membranes co-grafted with PEG and PIPAAm have been effectively applied to accelerate detachment of viable bovine aortic endothelial cell sheets from culture surfaces. Introduction of limited amount of PEG chains on the microporous culture surfaces had no adverse effect on cell attachment or proliferation. It also allows rapid access and diffusion of water molecules from beneath as well as the periphery of the cultured cell sheets, facilitating rapid hydration of grafted PIPAAm chains and cell sheet detachment. Enhanced diffusion of water molecules by co-grafted PEG moiety permits dramatically rapid cell sheet detachment than PIPAAm-grafted porous membranes without PEG moiety. Rapid two-dimensional intact cell sheet recovery by reduced temperature should prove interesting to fabricate three-dimensional tissue-like structures by stratification of various types of cell sheets.

Acknowledgements

A part of this research was financially supported by the Japan Society for the Promotion of Science, "Research for the Future" Program (JSPS-RFTF96I00201) for the fiscal year of 2000, and the Grant-in-Aid for Scientific Research (Grant No. 13308055). The authors are grateful to Dr. T. Aoki of Sophia University (Tokyo, Japan) for providing them a chance for ESCA measurements.

References

[1] Yamada N, Okano T, Sakai H, Karikusa F, Sawasaki Y, Sakurai Y. Thermo-responsive polymeric surfaces; control of attachment and detachment of cultured cells. Makromol Chem Rapid Commun 1990;11:571–6.

[2] Okano T, Yamada N, Sakai H, Sakurai Y. A novel recovery system for cultured cells using plasma-treated polystyrene dishes grafted with poly(*N*-isopropylacrylamide). J Biomed Mater Res 1993;27:1243–51.

[3] Okano T, Yamada N, Okuhara M, Sakai H, Sakurai Y. Mechanism of cell detachment from temperature-modulated, hydrophilic–hydrophobic polymer surfaces. Biomaterials 1995;16:297–303.

[4] Kikuchi A, Okuhara M, Karikusa F, Sakurai Y, Okano T. Two-dimensional manipulation of confluently cultured vascular endothelial cells using temperature-responsive poly(*N*-isopropylacrylamide)-grafted surfaces. J Biomater Sci Polym Ed 1998;9(12):1331–48.

[5] Kushida A, Yamato M, Konno C, Kikuchi A, Sakurai Y, Okano T. Decrease in culture temperature releases monolayer endothelial cell sheets together with deposited fibronectin matrix from temperature-responsive culture surfaces. J Biomed Mater Res 1999;45:355–62.

[6] Heskins M, Guillet JE, James E. Solution properties of poly(*N*-isopropylacrylamide). J Macromol Sci Chem A 1968;2:1441–5.

[7] Takei YG, Aoki T, Sanui K, Ogata N, Sakurai Y, Okano T. Dynamic contact angle measurement of temperature-responsive surface properties for poly(*N*-isopropylacrylamide) grafted surfaces. Macromolecules 1994;27(21):6163–6.

[8] Yakushiji T, Sakai K, Kikuchi A, Aoyagi T, Sakurai Y, Okano T. Graft architectural effects on thermo-responsive wettability changes of poly(*N*-isopropylacrylamide)-modified surfaces. Langmuir 1998;14(16):4657–62.

[9] Hirose M, Kwon OH, Yamato M, Kikuchi A, Okano T. Creation of designed shape cell sheets that are noninvasively harvested and moved onto another surface. Biomacromolecules 2000;1(3):377–81.

[10] Kushida A, Yamato M, Kikuchi A, Okano T. Two-dimensional manipulation of differentiated Madin–Darby canine kidney (MDCK) cell sheets: the non invasive harvest from temperature-responsive culture dishes and transfer to other surfaces. J Biomed Mater Res 2001;54(1):37–46.

[11] Kwon OH, Kikuchi A, Yamato M, Okano T. Rapid cell sheet detachment from poly(*N*-isopropylacrylamide)-grafted porous cell culture membranes. J Biomed Mater Res 2000;50:82–9.

[12] Kaneko Y, Nakamura S, Sakai K, Kikuchi A, Aoyagi T, Sakurai Y, Okano T. Deswelling mechanism for comb-type grafted poly(*N*-isopropylacrylamide) hydrogels with temperature responses. Polym Gels Networks 1998;6:333–45.

[13] Kaneko Y, Nakamura S, Sakai K, Aoyagi T, Kikuchi A, Sakurai Y, Okano T. Rapid deswelling response of poly(*N*-isopropylacrylamide) hydrogels by the formation of water release channels using poly(ethylene oxide) graft chains. Macromolecules 1998;31(18):6099–105.

[14] Tamada Y, Ikada Y. Fibroblast growth on polymer surfaces and biosynthesis of collagen. J Biomed Mater Res 1994;28:783–9.

[15] Lee JH, Lee SJ, Khang G, Lee HB. Interaction of fibroblasts on polycarbonate membrane surfaces with different micropore sizes and hydrophilicity. J Biomater Sci Polym Ed 1999;10(3):283–94.

[16] Merill EW, Salzman EW. Polyethylene oxide as a biomaterial. Trans-Am Soc Artif Intern Organs 1983;6:60–6.

[17] Harris JM. Introduction to biotechnical and biomedical applications of poly(ethylene glycol). In: Harris JM, editor. Poly(ethylene glycol) chemistry: biotechnical and biomedical applications. New York: Plenum Press, 1992 [chapter 1].

[18] Morra M, Occhiello E, Garbassi F. Surface modification of blood contacting polymers by poly(ethylene oxide). Clin Mater 1993;14:255–65.

[19] Silver JH, Myers CW, Lim F, Cooper SL. Effect of polyol molecular weight on the physical properties and haemocompatibility of polyurethanes containing polyethylene oxide macrogels. Biomaterials 1994;15:695–704.

[20] Han DK, Park KD, Ryu GH, Kim UY, Min BG, Kim YH. Plasma protein adsorption to sulfonated poly(ethylene oxide)-grafted polyurethane surface. J Biomed Mater Res 1996;30:23–30.

[21] Castillo EJ, Koenig JL, Anderson JM, Lo J. Protein adsorption on hydrogels. II. Reversible and irreversible interactions between lysozyme and contact lens surfaces. Biomaterials 1986;6:338–45.

[22] Lee JH, Kopeckova P, Zhang J, Kopecek J, Andrade JD. Protein resistance of polyethylene oxide surfaces. ACS Polym Mater: Sci Eng 1988;59:234–8.

[23] Andrade JD, Nagaoka S, Cooper S, Okano T, Kim SW. Surfaces and blood compatibility: current hypothesis. Trans-Am Soc Artif Intern Organs 1987;33:75–84.

[24] Nagaoka S, Nakao A. Clinical application of antithrombogenic hydrogel with long poly(ethylene oxide) chains. Biomaterials 1990;11:119–21.
[25] Nagaoka S, Mori Y, Takiuchi H, Yokota K, Tanzawa H, Nishiumi S. Interaction between blood components and hydrogels with poly(oxyethylene) chains. ACS Polym Prep 1983;24:67–8.
[26] Nagaoka S, Mori Y, Takiuchi H, Yokota K, Tanzawa H, Nishiumi S. Interaction between blood components and hydrogels with poly(oxyethylene) chains. In: Shalaby SW, Hoffman AS, Ratner BD, Horbett TA, editors. Polymers as biomaterials. New York: Plenum Press, 1984. p. 361–74.
[27] Nakayama Y, Miyamura M, Hirano Y, Matsuda T. Preparation of poly(ethylene glycol)-polystyrene block copolymers using photochemistry of dithiocarbamate as a reduced cell-adhesive coating material. Biomaterials 1999;20:963–70.
[28] Yamato M, Konno C, Kushida A, Hirose M, Utsumi M, Kikuchi A, Okano T. Release of adsorbed fibronectin from temperature-responsive culture surfaces requires cellular activity. Biomaterials 2000;21:981–6.
[29] Yamato M, Utsumi M, Kushida A, Konno C, Kikuchi A, Okano T. Thermo-responsive culture dishes allow the intact harvest of multilayered keratinocyte sheets without dispase by reducing temperature. Tissue Eng 2001;7(4):473–80.
[30] Takezawa T, Mori Y, Yoshizato K. Cell culture on a thermo-responsive polymer surface. Bio/Technol 1990;8:854–6.
[31] Yamato M, Kikuchi A, Kohsaka S, Terasaki T, vonRecum HA, Kim SW, Sakurai Y. Novel manipulation technology of cell sheets for tissue engineering. In: Ikada Y, Okano T, editors. Tissue engineering for therapeutic use 3. Amsterdam: Elsevier, 1999. p. 99–107.

Artificial Organs
27(1):84–91, Blackwell Publishing, Inc.

Investigation on the Mechanical Properties of Contracted Collagen Gels as a Scaffold for Tissue Engineering

*Z. Feng, †M. Yamato, ‡T. Akutsu, *T. Nakamura, †T. Okano, and ‡M. Umezu

**Department of Bio-System Engineering, Faculty of Engineering, Yamagata University, Yonezawa; †Institute of Advanced Biomedical Engineering and Science, Tokyo Women's Medical University; and ‡Department of Mechanical Engineering, Faculty of Engineering, Waseda University, Tokyo, Japan*

Abstract: In this article the mechanical properties of contracted collagen gels were investigated thoroughly by means of uniaxial tensile test. Large type I collagen-Dulbecco's Modified Eagle Medium (DMEM) gels (each was 26 ml in volume, 1.67 mg/ml collagen concentration), each populated with about 2.5×10^6 human fibroblasts, were made in 100 mm diameter plastic dishes precoated with albumin for floating the gels in DMEM. Such identically treated gels were divided into three groups for the mechanical measurements at different culture periods (2, 4, and 10 weeks). Rapid contraction occurred within the first 3 days and then the contraction went slowly in the rest period until it reached about 13% of its original size. The stress-strain curve of the contracted collagen gels demonstrated an exponential behavior at low stress region, followed by linear region, a point of yielding, and finally an ultimate stress point at which the maximum stress was reached. The mechanical strength increased in the first few weeks and then decreased as the culture went on. It is obvious that the collagen fibrils formed and were forced to orientate to the tensile direction after the test. The stress relaxation and cyclic creep phenomena were observed. Based on the morphological analysis of transmission electron microscopy (TEM) of the gels, a nonlinear visco-elastic-plastic constitutive formula was proposed, which was able to reproduce the rheological phenomena of the gels. This experiment shows that the human fibroblasts significantly contracted collagen gels so as to achieve certain mechanical strength, which makes it possible to be a scaffold for tissue engineering. However, a further method to reinforce the mechanical strength by several folds must be considered. Meanwhile, the rheological phenomena should be taken into account in the fabrication and application of the structure. **Key Words:** Collagen type I—Contracted collagen gel—Human fibroblast—Mechanical properties—Rheological properties—Tissue engineering.

Collagen constitutes the greatest quantity of the total proteins in the human body, and is the major composition of extracellular matrix and provides the tensile strength in tissues. In tissue engineering, the attractive and excitingly developing field that applies the principles of engineering and life sciences toward the construction of biological substitutes, it is so natural that collagen is used as a scaffold for developing those substitutes, particularly for blood vessel graft (1–3), artificial skin (4), ligament (5), and tendon (6), where at the first stage, cells are dispersed into a collagen-based cell suspension and cast into gels.

Meanwhile, it was found that collagen gels could be contracted as populated with some cells (7–9). This process is thought to be related to tissue remodeling and is characterized as that collagen matrix is accumulated by some integrins of the embedded cells to their vicinity and such accumulating traction is finally sustained by cytoskeleton (10–12). This contraction phenomenon occurs exclusively when collagen gels act as scaffolds in the above applications in tissue engineering.

Gel contraction makes collagen density increase so as to elevate mechanical strength. However, for the sake of required shapes of engineered substitutes, this contraction is usually constricted to a certain extent so that the data about its mechanical strength

Received September 2002.
Presented in part at the 3rd Japan–Australia Cardiovascular Bioengineering Symposium, held November 9–10, 2001 in Sendai, Japan.
Address correspondence and reprint requests to Dr. Zhonggang Feng, Nakamura Laboratory, Department of Bio-System Engineering, Yamagata University, 4-3-16, Joh-Nan, Yonezawa 992-8510, Japan. E-mail: zhgfeng@yz.yamagata-u.ac.jp

is tested in definite conditions and is not able to reflect the relationship between mechanical strength and contraction status (1,3). Furthermore, it is not difficult to imagine that such contracted collagen gels must present some rheological characteristics because collagen-rich tissues in our bodies have shown them. The rheological properties are of importance for the collagen-based structures, particularly for that cultured in a continuous tensile circumstance such as in some tensile bioreactor (13,14). Unfortunately, there is little data to show these properties and what the differences are between tissue engineered collagen-based structure and collagen-rich tissues in vivo.

In this research, we tested out the mechanical strengths of large collagen gels populated with human fibroblasts that spanned the whole free-contraction course. Moreover, the rheological properties of the contracted collagen gels were investigated in detail, and a nonlinear formula was proposed to regress their rheological phenomena.

MATERIALS AND METHODS

Materials

Type I collagen solution (8 mL) in distilled water (5 mg/ml porcine collagen, dissolved by HCl, Koken Ltd., Tokyo, Japan) was mixed with 12 ml 1× DMEM (Dulbecco's Modified Eagle's Medium, supplemented with 10% fetal bovine serum and 100 U/ml penicillin) and 4 ml 3× DMEM so that the final mixture resulted in a 1.67 mg/ml collagen solution of 1× DMEM with a physiological ionic strength. Human fibroblast (28th passage, 2 mL) (TIG, provided by Riken Cell Bank, Tokyo, Japan) in 1× DMEM including 2.5×10^6 cells were added into the above collagen solution and mixed thoroughly. This process was performed on ice to prevent early gel formation. Finally, this mixture was poured into a 100 mm diameter plastic dish (Becton Dickinson Company, Franklin Lakes, NJ, U.S.A.) coated with albumin and was allowed to gel at 37°C for 60 min. After gelation, 10 ml 1× DMEM was added to float the gel and then it was cultured in a CO_2 incubator. Medium changes were performed every 3 days. Twelve such identically treated gels were made and divided into three groups for the mechanical measurements at different culture periods (2, 4, and 10 weeks). To assay the gel contraction, we measured the diameters of the gels in two perpendicular directions and gave out the average data, which were ultimately expressed as the percentage of the original diameter, and each data point was calculated by taking the average of all gels.

Uniaxial tensile test

Test specimen

The size of the cultured collagen gels after contraction decreased to about 15 mm diameter by 0.3 mm thickness. Figure 1 shows the specimen preparation for uniaxial tensile test. The test-piece was cut into a gauge length and width of 9 mm and 5 mm, respectively. The two ends of the piece were sewed with two envelope paper strips to be held by the test rig. The remaining parts of the collagen gel were kept for histological studies as the pretest sample.

Test rig

The uniaxial tensile tests were carried out using a conventional testing machine (AUTOGRAPH AG-B, Shimadzu Co., Kyoto, Japan) equipped with two sample grips and a 50 N load cell (SBL-50N). The minimal measuring range (0–50 g) of the load cell was employed in the tests. Figure 2 shows the schematic drawing of the rig. The specimen sinking in DMEM bath was held by two grips. The upper grip is connected to the load cell and can make a reciprocating movement. The force applied on the specimen is measured by the load cell and transmitted into tension later; meanwhile the displacement sensor can detect the movement of the upper grip and thereby the strain of the tissue can be obtained. In the tests, the measurements of force and displacement were sampled into a computer and were converted to stress and strain. The stress-strain curves were plotted on an X–Y graph recorder.

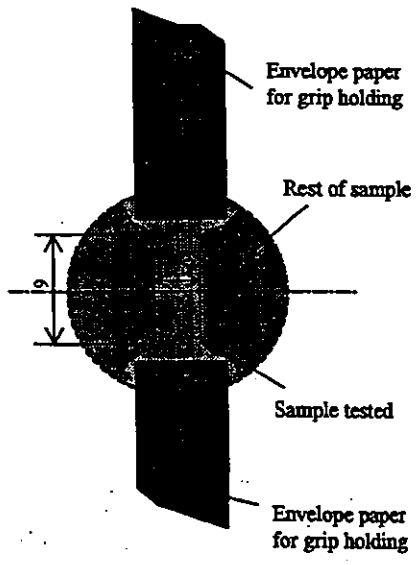

FIG. 1. The drawing shows a sample for the uniaxial mechanical test.

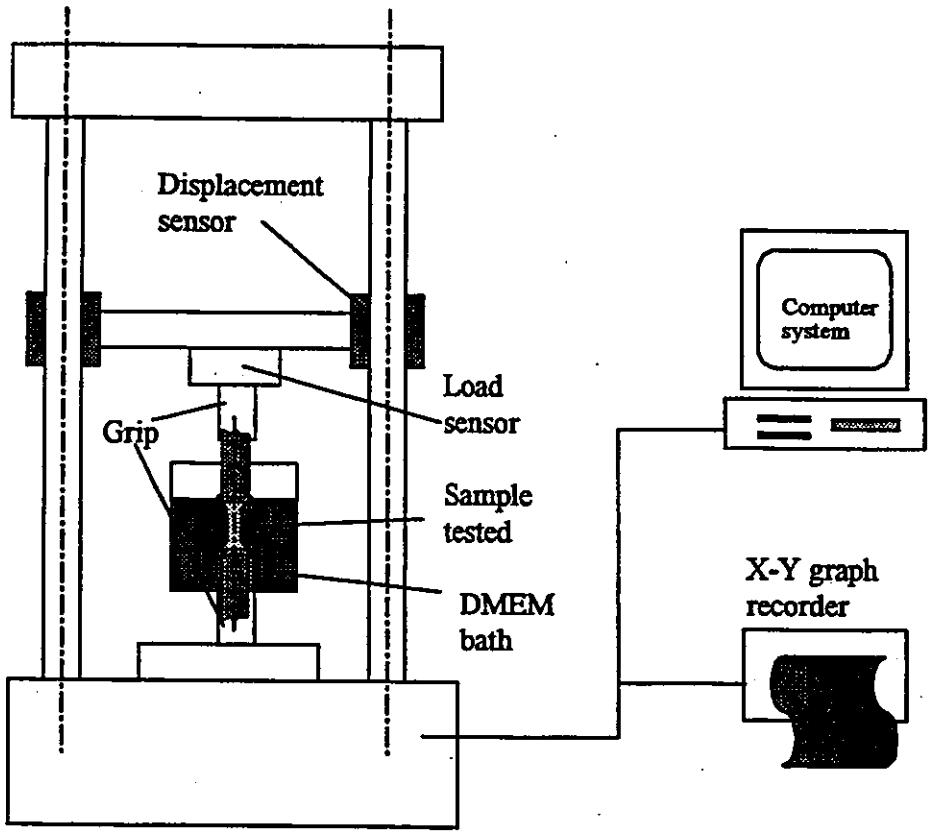

FIG. 2. A test rig of uniaxial mechanical properties is shown.

Strength test

The test specimen was first preconditioned by cyclic loading. The maximal precondition load was set at 5 g (33.3 kPa apparent stress) and the strain rate was 0.009 per second. All specimens were preconditioned for 10 loading cycles. After the precondition, the sample got 3 min relaxation and was then stretched until broken at strain rate 0.009 per second.

Rheological test

The rheological test was conducted only on 4 week samples. After the preconditioning, the stress relaxation test and cyclic creep test were performed serially.

In the stress relaxation test, the sample was stretched to 10 g tensile (66.7 kPa apparent stress) obtained, and then the upper rig stopped moving to keep the strain constant, and the stress decayed, i.e., stress relaxation phenomenon presented. After, the cyclic creep test was done. The sample was loaded to 10 g tensile (66.7 kPa apparent stress) at 0.0009/s strain rate and then unloaded immediately at the same strain rate. The process was conducted cyclically and the variation of the maximal strain at every loading cycle, i.e., cyclic creep phenomenon, was recorded.

Histological studies

The gel samples before and after the tensile test were fixed for transmission electron microscopy. Specimens were fixed overnight by 4% glutaraldehyde in PBS, pH 7.4. Sections were cut in the direction of tensile load and were stained using standard techniques (carried out by Kawasaki Institute for Histology, Tokyo, Japan).

RESULTS

Collagen gel contraction

Coinciding with the existing results (15), this study showed that human fibroblasts were able to contract the collagen gels significantly. Figure 3 shows the contractions of a gel at 0, 1, and 14 day incubation, respectively. Figure 4 gives the time course of the collagen gel contraction. It can be seen that the rapid contraction occurred within the first 3 days, and then the contraction took place slowly in the rest period to a final diameter of about 13% of its original size. It is noteworthy that after two weeks' incubation, the gels began to wrinkle and finally contracted to a ball-like outward shape of about 10 mm diameter, which could be flattened to a sheet when mechanical tests were performed.

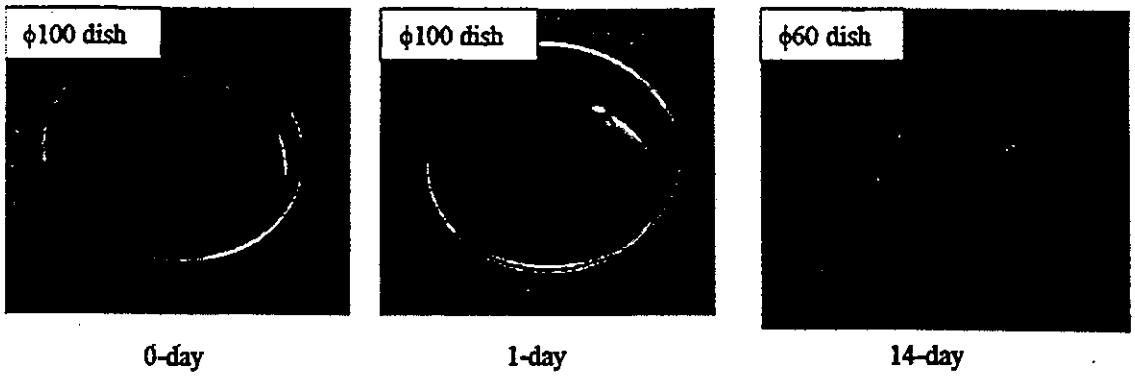

FIG. 3. Contractions of human fibroblasts populated-collagen gels are illustrated.

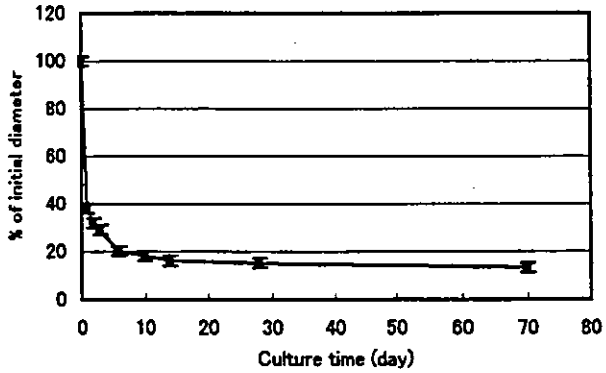

FIG. 4. The graph shows the time course of collagen gels contraction.

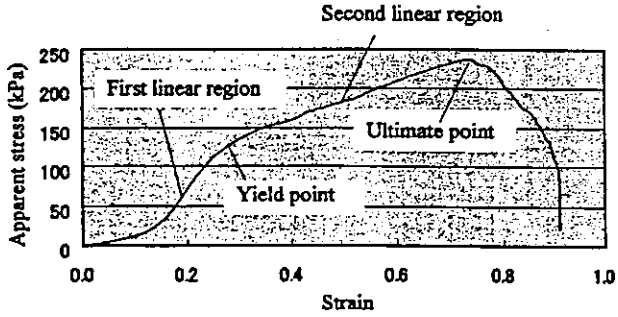

FIG. 5. The graph illustrates the typical stress-strain relation of contracted collagen gels, cultured for two weeks.

Mechanical properties

The collagen gels were tested at 2, 4, and 10 week culture, respectively. Figure 5 shows a typical stress-strain curve up to failure of a gel cultured for two weeks. The horizontal axis is tensile strain corresponding to the original length (9 mm) of the specimen and the vertical axis is the stress. The reason why we express the stress as "apparent stress" is because the width and thickness of the sample got smaller than its original data due to the preconditioning elongation and during the test performed, whereas the stress was still calculated using the original morphological data. This stress-strain curve presented some common features for connective tissue (16), in that it demonstrated an exponential behavior at low stress region, followed by a linear region, a point of yielding, and finally an ultimate stress point at which the maximum stress was reached. However, Fig. 5 shows another feature that should be noted, i.e., besides the linear region before the yield point, linear region after the yield point occurred, whereas there is commonly only one linear region before the yield point in the curve of connective tissue. We defined four parameters to describe the mechanical properties of the contracted collagen gel (see Fig. 5): first, yield point stress, which was defined as the stress deviating from the first linearity by 10%; second, ultimate stress, that is the maximal stress in the stress-strain curve; third, low stress modulus, that is slope of the first linear portion; and fourth, high stress modulus, that is slope of the second linear portion. Figures 6 and 7 present these parameters at the three different culture periods, respectively.

In Fig. 6, an important outcome was that the gel mechanical strength, i.e., yield stress and ultimate stress, reached the biggest amount at 4-week culture. The variation of the mechanical strength showed that it first increased and then decreased as culture went on. The same tendency was maintained in the parameters of low stress modulus and high stress modulus (see Fig. 7).

Rheological properties

The rheological tests were conducted only on 4 week specimens. Figure 8 shows their typical curves of stress relaxation and cyclic creep. In Fig. 8a, it can be seen that when this gel was loaded at a finite strain

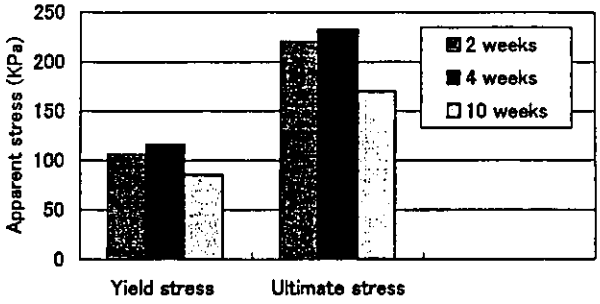

FIG. 6. Mechanical strengths of contracted collagen gels are shown.

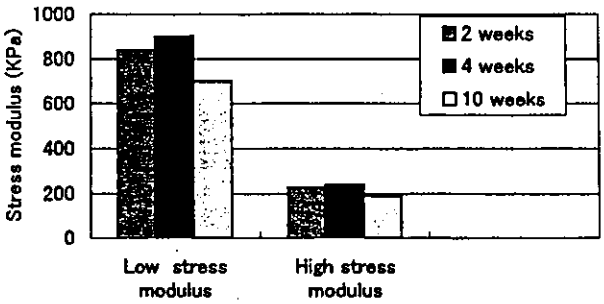

FIG. 7. Stress moduli of contracted collagen gels are shown.

rate to a certain stress (about one-fourth of its failure load) and then its length was held constant, the phenomenon of stress relaxation presented, and the stress relaxed asymptotically to a limiting value. In Fig. 8b, the specimen was loaded to about one-fourth of its failure load and then unloaded to zero immediately at a constant speed, and this process was repeated cycle by cycle. It can be seen that with every loading-unloading cycle, the gel was stretched a little bit longer than in the preceding cycle. This phenomenon is named "cyclic creep" since strain creep occurred in every cycle. This creep decreased with the loading cycle going on; however, it did not disappear by the twentieth cycle in our experiment.

Histological evaluation

Figures 9a–9c show the histological appearances of pre- and post-test of 4-week culture, and post-test of 10-week culture, respectively. First of all, it can be judged that collagen fibrils exhibited in these figures with the reference of size bar, and the cross striations of some fibrils could be observed on the original TEM pictures (rather than on these figures scanned into the article, which made them indistinct). The fibrils got thicker and the density increased more with the 10 week culture than with the 4 week (comparing Fig. 9a with c). Nevertheless, neither of them packed together to form bundles, that is to say, to form collagen fibers. Nothing implies the existence of cross-linking among the fibrils. Another difference in reference to in vitro collagen-rich tissue is that the fibrils are very short.

Comparing with Figs. 9a and b, we can see that after the mechanical tensile test, the randomly arranged fibrils were orientated along the direction of tensile load. This obvious topological variation makes sense since recovering ability of random arrangement of the fibril (some kind of elastic recovering) was so weak and the gel breaking resulted from fibrils sliding in magnitude.

DISCUSSION

Mechanical strength

Human fibroblasts contracting collagen lattice were reported in the late 1970s (15). Since then, some researchers had investigated the mechanical strength by means of a tensile test. Chapuis and Agache (17) investigated the variation of stiffness modulus (corresponding to the low stress modulus here) with culture duration and collagen and fibroblast concentrations. The stiffness modulus increased in 2 weeks' culture. Since the culture duration was not long enough, no peak value in stiffness modulus appeared. Correspondingly, the value of the modulus was in the same

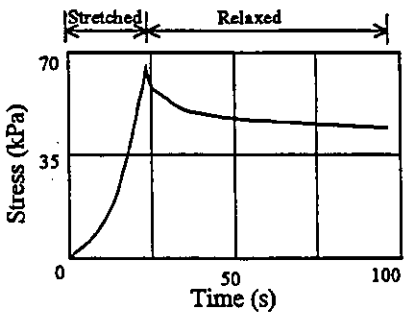

(a) Stress relaxation

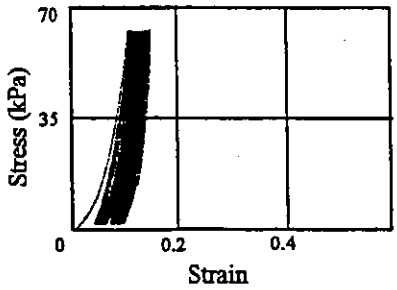

(b) Cyclic creep (20 cycles)

FIG. 8. Rheological properties of contracted collagen gels are shown; depicts stress relaxation (a) and illustrates cyclic creep (b).

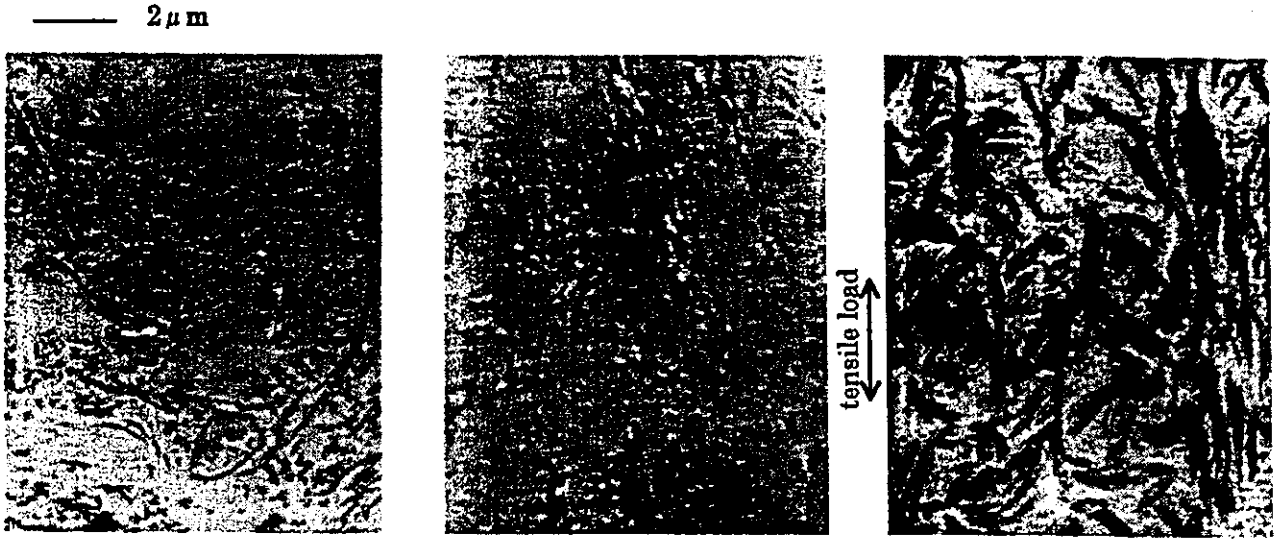

FIG. 9. Shown is the histological appearance of contracted collagen gels.

order but less than the data in this article. No second linear region presented in their stress-strain curves.

Huang et al. (18) measured the mechanical strength of long time cultured (up to 80 days) collagen gels populated by human dermal fibroblasts. A maximum of linear modulus exhibited around 60 day culture, but failure load increased in the entire culture duration. It may have been caused by the progression of the collagen contraction under tensile environment, and that the culture medium was further modified to enhance the incorporation between collagen and fibroblasts and the cross-linking among collagen fibrils. Therefore, the strength they reported is consistently higher than that of this experiment.

In this research, large gels were made intended for tissue engineering substrate and the gels contracted freely without any constriction. The data reflected primary characteristics of this structure and provided a reference for its further application. Because no cross-linking was induced, the mechanical strength will not continuously increase with the culture duration. Conversely, due to the increase of fibril's thickness and density, the viscous effect may decrease, as discussed in the following, and this is considered to result in a decrease of the mechanical strength in long-term culture. Therefore, how to induce collagen fibers formation and stimulate cross-linking among them is a critical way to reinforce the mechanical strength.

Collagen concentration and cell number have an impact on the mechanical strength according to other investigations (17), but the variation is limited within the same order and tends to decrease in long-term culture. In this research, the collagen concentration (1.67 mg/ml) was chosen at a middle value in its conventional alteration range, and moreover, this collagen concentration and seeded cell number (2.5×10^6) were close to those for tissue engineered artificial vessels (1,3). Therefore, the contracted collagen gels made in these parameters were considered to be representative.

Rheological properties

The phenomenon of stress relaxation has been observed in the samples of natural connective tissue, and as for the cyclic loading test, the stress-strain relation exhibits a close curve with hysteresis and can be found to shift with different loading cycles (16). However, no cyclic creep occurred as happened in this experiment. The microstructure of the contracted collagen gels, as shown in Fig. 9, was relatively simple compared with collagen-rich tissue in vivo. Regardless of the substructure near the populated-fibroblasts, the contracted gels can be considered a random arrangement, therefore an isotropic material, of collagen molecules and fibrils lacking cross-linking.

Under the tensile load the molecules and fibrils would be first stretched out, and then as the load increased the orientation and sliding of the fibrils took place. The stretching out and some part of the orientation were of elastic property and could

recover with unloading, but most parts of the orientation and the whole sliding were of plastic and viscous features, and they could not be recovered by unloading. Because of the lack of cross-linking here, the sliding happened when the gel was standing for a very small load that was postulated to be the turning point into the first linear region in the stress-strain curve.

The unrecoverable strain in the cyclic loading test resulted in the cyclic creep. By such understanding, we proposed a nonlinear visco-elastic-plastic constitutive formula to analyze the stress-strain behaviors in the experiment:

$$\sigma = E(\gamma)\cdot\gamma + (\eta/\lambda)\int_{\gamma_0}^{\gamma} e^{-[\gamma(\gamma)-\gamma(\gamma')]/\lambda} d\gamma', \qquad (1)$$

where σ, γ, and t represent stress, strain, and deformation time, respectively, and η and λ are sliding viscosity and relaxation time, respectively. $E(\gamma)\cdot\gamma$ is nonlinear elastic-plastic term. Here strain γ_0 is an important parameter, at which the sliding started.

Figure 10 gives the stress-strain relation by means of Eq. 1 and the nonlinear elastic-plastic and viscous portions in it, respectively. Here the nonlinear elastic-plastic term $E(\gamma)\cdot\gamma$ was expressed as $Ee\cdot\gamma^2/(\gamma^2 + b\cdot\gamma + c)$. It had a maximal limit as shown in Fig. 10, which meant that after a certain strain γ_1 reached, the stress-strain relation of this portion entered a quasi-plastic zone and the increment of the stress was almost contributed by the nonlinear viscous term; γ_1 was therefore the yield strain.

The nonlinear viscous term $(\eta/\lambda)\int_{\gamma_0}^{\gamma} e^{-[\gamma(\gamma)-\gamma(\gamma')]/\lambda} d\gamma'$ was virtually of memory property, which meant the stress status at present was determined wholly by its strain history. This memory-owing constitutive relation had been employed to describe the rheological phenomena under large deformation conditions and proved to be effective in depicting hysteresis features (19).

By means of Eq. (1), we can also describe the phenomena of stress relaxation and cyclic creep of the contracted collagen gels, as shown in Fig. 11. It can be seen that these two rheological features are depicted with good agreement with the experimental data. Through a further analysis of Fig. 11 and Eq. (1), we can see that the relaxation of stress was actually due to the decay of nonlinear viscous term and the cyclic creep was due to the memory effect of the term. The reason the mechanical strength decreased as the culture continued a long time is because viscous effect decreased. Actually, the yield and ultimate strains of 10 week samples were both less than those of 4 week ones (data not shown here).

Nowadays, researchers emphasize the vital role of tensile environment in the fabrication of tissue-engineered organs (2,3,13,14). Therefore, the rheological properties are of importance both in the fabrication of the collagen-based structure and in its application in vivo, because in both cases the continuous loading imposes the structure. In this test, we revealed the rheological characteristics of the contracted collagen gel and proposed a nonlinear

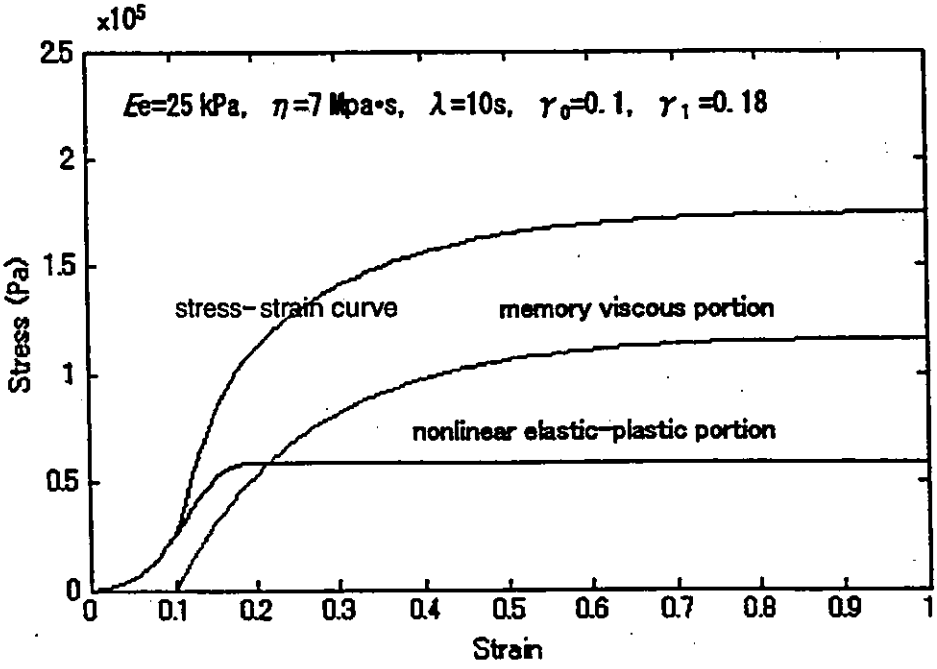

FIG. 10. The stress-strain relation depicted by constitutive formula is shown.

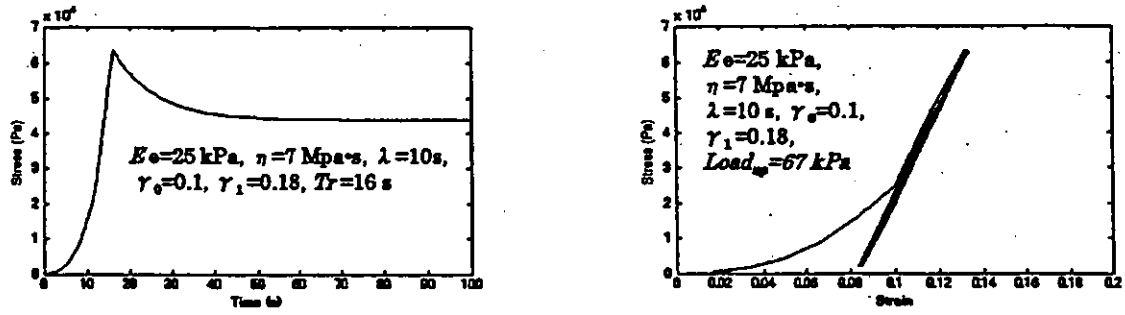

(a) Stress relaxation

(b) Cyclic creep (3 cycles computed)

FIG. 11. Rheological properties, stress relaxation (a) and cyclic creep (b), reproduced by constitutive formula are illustrated.

visco-elastic formula to regress them. It is very helpful to guide the fabrication and application of the contracted collagen-based structure in tissue engineering.

REFERENCES

1. Weinberg CB, Bell E. A blood vessel model constructed from collagen and cultured vascular cells. *Science* 1986;231:397–400.
2. Kanda K, Matusda T. Mechanical stress-induced orientation and ultrastructure change of smooth muscle cells cultured in three-dimentional collagen lattices. *Cell Transplant* 1994;3: 481–92.
3. Seliktar D, Black RA, Vito RP, Nerem RM. Dynamic mechanical conditioning of collagen-gel blood vessel constructs induced remodeling in vitro. *Ann Biomed Eng* 2000;28:351–62.
4. Morimoto N, Suzuki S, Kim BM, Morota K, Takahashi Y, Nishimura Y. In vivo cultured skin composed of two-layer collagen sponges with preconfluent cells. *Ann Plast Surg* 2001;47:74–82.
5. Kuboki Y, Sasaki M, Saito A, Takita H, Kato H. Regeneration of periodontal ligament and cementum by BMP-applied tissue engineering. *Eur J Oral Sci* 1998;106(Suppl 1):197–203.
6. Ker RF. The design of soft collagenous load-bearing tissues. *J Exp Biol* 1999;202:23:3315–24.
7. Tiollier J, Dumas H, Tardy M, Tayot J. Fibroblast behavior on gels of type I, III, and IV human placental collagen. *Exp Cell Res* 1990;191:95–104.
8. Vernon RB, Sage EH. Contraction of fibrillar type I collagen by endothelial cells: A study in vitro. *J Cell Biochem* 1996;60:185–97.
9. Liu X, Umino T, Cano M, Ertl R, Veys T, Spurzem J, Romberger D, Rennard S. Human bronchial epithelial cells can contract type I collagen gels. *Am J Physiol* 1998;274(Lung Cell. Mol. Physiol. 18):L58–L65.
10. Steinberg BM, Smith K, Colozzo M, Pollack R. Establishment and transformation diminish the ability of fibroblasts to contract a native collagen gel. *J Cell Biol* 1980;87:304–8.
11. Burridge K, Fath K, Kelly T, Nuckolls G, Turner C. Focal adhesions: transmembrane junctions between the extracellular matrix and the cytoskeleton. *Annu Rev Cell Biol* 1988;4: 487–525.
12. Yamato M, Hayashi T. Topological distribution of collagen binding sites on fibroblasts cultured within collagen gels: Extracellular matrix-cellular interaction. In: Ninomiya Y et al., eds. *Molecules to Disease*. Tokyo: Japan Sci. Soc. Press, Basel S. Karger, 1998:123–40.
13. Cacou C, Palmer D, Lee DA, Bader DL, Shelton JC. A system for monitoring the response of uniaxial strain on cell seeded collagen gels. *Med Eng Physics* 2000;22:327–33.
14. Langelier E, Rancourt D, Bouchard S, Lord C, Stevens PP, Germain L, Auger FA. Cyclic traction machine for long-term culture of fibroblast-populated collagen gels. *Ann Biomed Eng* 1999;27:67–72.
15. Bell E, Ivarsson B, Merril C. Production of a tissue-like structure by contraction of collagen lattices by human fibroblasts of different proliferation potential in vitro. *Proc Natl Acad Sci USA* 1979;76:1274–8.
16. Fung YC. *Biomechanics: Mechanical properties of living tissue*, 2nd edition. New York: Springer-Verlag, Inc., 1993.
17. Chapuis JF, Agache P. A new technique to study the mechanical properties of collagen lattices. *J Biomechanics* 1992;25:115–20.
18. Huang D, Chang TR, Aggarwal A, Lee RC, Ehrlich HP. Mechanisms and dynamics of mechanical strengthening in ligament-equivalent fibroblast-populated collagen matrices. *Ann Biomed Eng* 1993;21:289–305.
19. Schowalter WR. *Mechanics of non-Newtonian fluids*, Oxford: Pergamon Press, 1978.